Engineering Perspective 4 (1): 7-16, 2024

e-ISSN:2757-9077

ENGINEERING PERSPECTIVE

https://sciperspective.com/

Research Paper

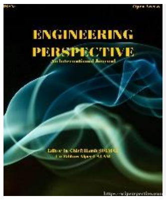

Integrated Vehicle Dynamics Modeling, Path tracking, and Simulation: A MATLAB Implementation Approach

Fatima Haidar[1*], Abderaouf Laib[1], Syed Ali Ajwad[1], Guillaume Guilbert[1]

[1] *Capgemini Engineering, Research & Innovation Direction, 12 rue de la Verrerie, 92190, Meudon, France*

ABSTRACT

This paper presents a thorough exploration of vehicle dynamics modeling and simulation, focusing on lateral, longitudinal, and vertical motion. A comprehensive mathematical representation of a car-like vehicle is developed, incorporating both kinematic and dynamic models to accurately capture its behavior. Initially, a kinematic model is established to describe fundamental motion in a 2D plane, while a subsequent dynamic model considers various forces influencing the vehicle's motion in a 3D space. The vertical motion of the vehicle is primarily influenced by its suspension systems. In this paper, we initially introduced a fundamental 2 Degree of Freedom (DOF) quarter car suspension model and subsequently presented a more comprehensive half car suspension model which accounts for both the front and rear body parts of the vehicle. The developed models are implemented using MATLAB/Simulink, enabling rigorous testing and validation of their accuracy. Simulation results demonstrate the precision of the developed models, consistently aligning with expected vehicle behavior under different input conditions. Specifically, the models accurately replicate vehicle motion in straight lines and circular patterns, corresponding to longitudinal speed and steering angle inputs. Additionally, a path tracking controller is integrated to showcase the model's efficiency and validate its derived parameters. The reliability and accuracy of the thoroughly developed models underscore their suitability for algorithm development and validation, essential for advancing autonomous vehicle technology and enhancing vehicle safety and performance.

Keywords: Autonomous vehicle; Mathematical modelling; Trajectory tracking; Vehicle dynamics.

History
Received: 14.12.2023
Accepted: 27.01.2024

Author Contacts
Corresponding Author
e-mail addresses : Fatima.haidar@capgemini.com, abderaouf.laib@capgemini.com, syed-ali.ajwad@capgemini.com, guillaume.guilbert@capgemini.com

How to cite this paper: Haidar, F., Laib, A., Ajwad, S.A., Guilbert, G., (2024). Integrated Vehicle Dynamics Modeling, Path tracking, and Simulation: A MATLAB Implementation Approach. Engineering Perspective, 4 (1), 7-16. http://dx.doi.org/10.29228/eng.pers.75106

1. Introduction

Since the last few decades, the automotive industry and the market structure has changed in an unprecedented way. There were simultaneous growing needs for vehicle safety, environmental protection, and intelligent control. As a result, the use of advanced technologies such as computer technologies, virtual reality technologies and intelligent algorithms became widespread in the industry. Thanks to these advanced technologies, the automotive industry focused on the design and testing of new Advanced Driving Assistance System (ADAS) functionalities to enhance not only the safety but also the performance and comfort of the vehicle and its passengers. The ADAS functionalities include lane keeping [1] but also adaptive cruise control [2], lane assistance [3], emergency braking [4], and parking assistance [5] among others. In recent times, fully Autonomous Driving (AD) is also becoming an increasingly interesting topic of research in the automotive industry [6] in which more advanced algorithms are required for trajectory planning and controlling.

Vehicle dynamics plays an important role in the automotive industry development [7]. The mathematical models not only allow to understand the behavior of the vehicle, but one can also use these models to verify and validate the developed algorithms in simulation before implementing them on the real hardware [8]. This allows a significant cost reduction. Moreover, by studying the complex interactions between a vehicle's components, such as its tires, suspension, and steering system, researchers can identify potential safety hazards and develop innovative solutions to improve vehicle safety [9].

Initially, research on vehicle dynamics focused on analyzing the vehicle's performance under various external conditions and service requirements. During the 1930s, there was a notable shift in research focus towards the steering, suspension mechanics, and driving stability of the vehicles [10]. Researchers like Lanchester Maurice and Segel began to examine how external environmental factors, such as road surface roughness, air flow, tire conditions, and driver behavior, impacted the vehicle dynamics. Additionally, they studied the interrelated effects of these various conditions [11]. In 1993, they provided a detailed overview of the progress made in vehicle dynamics research prior to 1990 in the Proceedings of Institution of Mechanical Engineers [12].

Over the subsequent decades, significant research has been devoted to investigating vehicle ride comfort and handling stability. The study of handling dynamics concerns primarily the lateral or transverse dynamics of the vehicle, including its handling, stability, vehicle sideslip resulting from tire lateral force, yawing, and roll motion. The research on vehicle handling stability in vehicle dynamics has evolved from experimental studies to theoretical analysis and from open-loop to closed-loop systems. The representative monographs of vehicle handling dynamics include "Vehicle Handling Dynamics Theory and Application" by Abe [13] and "Overview on Vehicle Dynamics" by Yang [7].

Vehicle driving dynamics is divided into two categories: longitudinal and lateral dynamics. Longitudinal dynamics concerns the motion of a vehicle along its longitudinal axis, which includes acceleration, braking, and the resulting changes in velocity. It also considers various resistive forces which influence the longitudinal movement of the vehicle [14]. Lateral dynamics on the other hand concerns the motion of a vehicle perpendicular to its longitudinal axis, which includes turning, cornering, and the resulting changes in direction. Both longitudinal and lateral dynamics are critical for vehicle handling, safety, and overall performance. Relevant monographs in this area can be found in "Vehicle Dynamics and Control" by Rajamani [15]. Another pivotal aspect of vehicle dynamics is the vertical motion regulated by the vehicle suspension system. Therefore, a comprehensive vehicle suspension mathematical model is of utmost importance to analyse and optimize the vehicle’s behaviour. This model not only profoundly influences the overall dynamics of the vehicle but also serves as a key component of vehicle stability, ride comfort, handling, and safety [16]. In recent times, researchers have also developed mathematical models not only for electric and hybrid powertrains and propulsion systems[17,18] but also for braking [14]and speed transmission systems [19]. However, it's crucial to highlight that vehicle motion dynamics models serve as pivotal components for testing and verifying these intricate models.

The main objective of this work is to create precise and efficient simulations by delving into key aspects of vehicle behavior. These aspects encompass lateral vehicle dynamics, longitudinal vehicle dynamics and vehicle suspension dynamics. The lateral vehicle dynamics pertains to the vehicle’s turning behavior, providing insights that enable the effective design of control systems. Longitudinal vehicle dynamics have been modeled to investigate acceleration, deceleration, and speed control responses to driver inputs and external factors. Furthermore, a vehicle suspension systems model has been developed to simulate the vehicle’s reaction to uneven road surfaces, therefore, enhancing ride comfort and stability, that are integral to passenger safety. Compared to the previous literature, this paper not only advances the understanding of the vehicle’s motion but also combines all three dynamics models to obtain a better analysis of the vehicle’s behavior in real driving scenarios, emphasizing safety considerations. A detailed derivation of these dynamics is provided in the paper. In the next step, these dynamics are implemented in MATLAB/Simulink. The implemented models are tested with various input signals. Finally, a path tracking controller is designed and implemented. The results of path tracking control show that the developed mathematical models mimic the real motion of a vehicle and can be used to design and validate algorithms for ADAS and AD in a simulation environment.

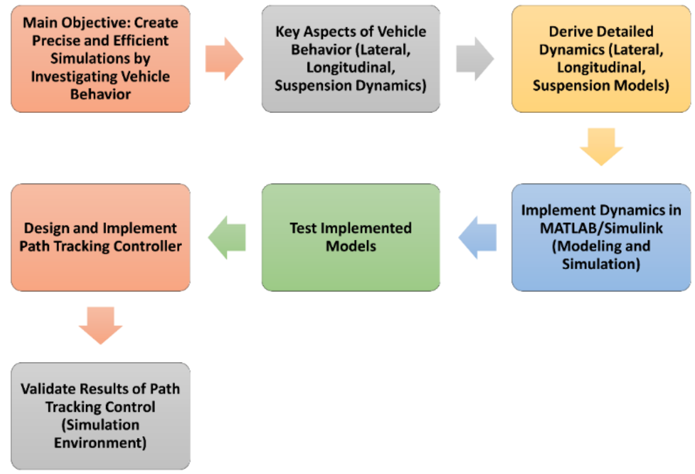

Figure 1. Flowchart summarizing the entire study.

The flowchart as shown in Figure 1 begins with the main objective of the study, which is to create precise and efficient simulations by investigating key aspects of vehicle behavior (section 1). It outlines the key aspects, including lateral, longitudinal, and suspension dynamics (section 2). The detailed dynamics are derived, implemented in MATLAB/Simulink, and tested with various input signals. A path tracking controller is designed and implemented (section 3), followed by the validation of results in a simulation environment (section 4).

2. Vehicle model description

This section discusses the derivation of vehicle mathematical modeling. First, the basic coordinate representation is described. Then both kinematic and dynamic models are discussed in detail.

2.1 Coordinate system

In vehicle dynamics, understanding coordinate systems is crucial for accurately analyzing the vehicle’s behavior. In order to develop the model, two coordinate frames are required i.e. the inertial frame and the body-fixed frame. The inertial frame is a reference frame that is fixed relative to the Earth's surface and does not move, while the vehicle frame is a reference frame that is fixed relative to the vehicle and moves with the vehicle's motion. Figure 2 depicts the reference coordinates. The parameters, which are the variable components essential in deriving the characteristics of the vehicle, are described beneath each corresponding equation.

Figure 2. Reference coordination.

2.2 Kinematic model

The kinematics of a 4-wheel vehicle can be simplified as 2-wheel bicycle model by merging the front and rear wheels. This reduces the complexity of dealing with 4 wheels and 2 steering angles to only 2 wheels and 1 steering angle. Let us consider that the body reference frame is at the center of gravity of the vehicle as shown in Figure 2. ψ describes the orientation of the vehicle, V is the velocity at the center of gravity and β is the slip angle.

The motion of the vehicle can then be described as in the Eq. (1) below:

$$\begin{cases} \dot{X} = V \ \cos(\psi + \beta) \\ \dot{Y} = V \ sine(\psi + \beta) \end{cases} \tag{1}$$

While the angular speed $\dot{\boldsymbol{\psi}}$ can be given as:

$$\dot{\psi} = \frac{V}{R} \tag{2}$$

Where R is the perpendicular distance from the reference point to the Instantaneous Center of Rotation (ICR) represented in Figure 3 as O.

Using basic angle geometry, it can be found that the intersecting angle between the front and rear perpendicular lines is equal to δ, thus leading to the following Eq. (3):

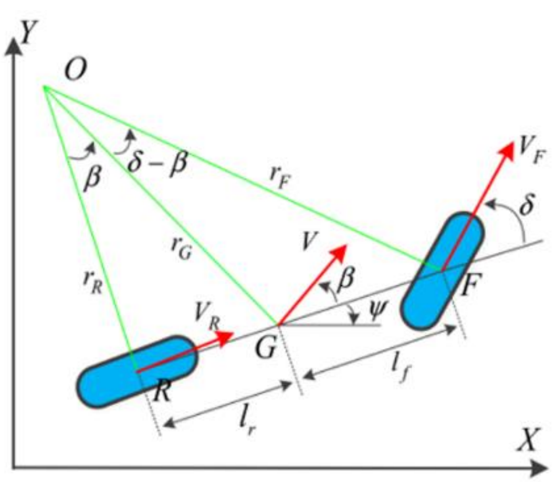

Figure 3. Two-wheel bicycle model [20].

$$\tan(\delta) = \frac{l_f + l_r}{r_R}, \tan(\beta) = \frac{l_r}{r_R} \tag{3}$$

Where l_r and l_f are the distances between the center of gravity and the rear and front axles respectively, r_R represent the distance between O to center of rear axle. From the above equations, the following Eq. (4) is obtained:

$$\begin{cases} \dot{\psi} = \dfrac{V}{l_r + l_f} cos(\beta)\, tan(\delta) \\ \beta = arctg\left(\dfrac{l_r}{l_r + l_f} \ \ tan(\delta)\right) \end{cases} \tag{4}$$

Eq. (1) and Eq. (4) combined describe the kinematics of the vehicle.

2.3 Dynamic model

In order to keep the model simple, some key assumptions were made. First, the vehicle is considered as a rigid body, whose dynamics is determined by the fundamental laws of motion. Second, the steering angle is small, which allows us to make the small-angle approximations such as $\cos(\delta) \approx 1$ and $\sin(\delta) \approx 0$.

- ***Lateral Dynamics***

Let us consider the free body diagram shown in Figure 4. According to Newton's second law:

$$\sum F = ma \quad \text{and} \quad \sum M = Iz \ \ddot{\Psi} \tag{5}$$

Where $\sum F$ represent the sum of forces, m represents the vehicle mass and a represent the vehicle acceleration. As well as $\sum M$ represent the sum of all moments, Iz represents the moment of inertia and $\ddot{\Psi}$ represents the angular acceleration of the vehicle.

Considering the lateral forces on front and rear tires in the small-angle approximation. The lateral acceleration is a combination of $\dot{V}_y$, which is due to the motion along the y axis, and $\ddot{\Psi} V_x$, referred to as centripetal acceleration. Therefore, the following Eq. (6) is obtained:

$$F_{yf} + F_{yr} = m(\dot{V}_y + \ddot{\Psi} V_x) \tag{6}$$

Now taking the moment around the center of gravity G:

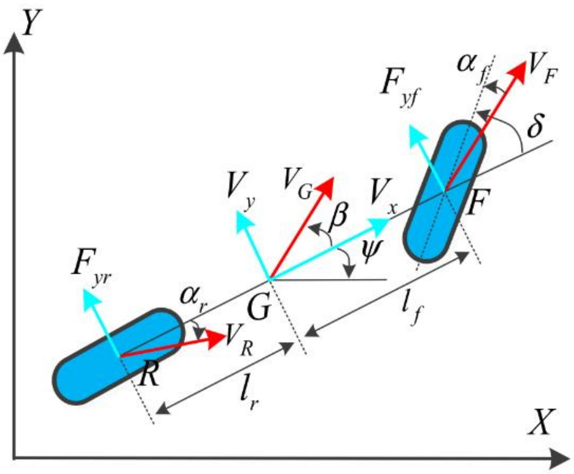

Figure 4. Free body diagram [20].

$$F_{yf} l_f - F_{yr} l_r = I_z \ddot{\Psi} \tag{7}$$

The slip angle of front and rear tire can be expressed as:

$$\alpha_f = \delta - \frac{V_y + l_f \dot{\varphi}}{V_x} \text{ and } \alpha_r = \frac{V_y - l_r \dot{\varphi}}{V_x} \tag{8}$$

Using the cornering stiffness of the tire, F_{yf} and F_{yr} are expressed as in the following Eq. (9):

$$F_{yf} = C_f \alpha_f \text{ and } F_{yr} = -C_r \alpha_r \tag{9}$$

Combining all above equations, the lateral model in the state-space can be represented as in Eq. (10):

$$\frac{d}{dt}\begin{bmatrix} Y \\ \dot{Y} \\ \psi \\ \dot{\psi} \end{bmatrix} = \begin{bmatrix} 0 & 1 & 0 & 0 \\ 0 & -\frac{c_f + c_r}{mV_x} & 0 & -(V_x + \frac{c_f l_f - c_r l_r}{mV_x}) \\ 0 & 0 & 0 & 1 \\ 0 & -\frac{c_f l_f - c_r l_r}{I_z V_x} & 0 & -\frac{l_f^2 c_f + l_r^2 c_r}{I_z V_x} \end{bmatrix} \times \begin{bmatrix} Y \\ \dot{Y} \\ \psi \\ \dot{\psi} \end{bmatrix} + \begin{bmatrix} 0 \\ \frac{c_f}{m} \\ 0 \\ \frac{c_f l_f}{I_z} \end{bmatrix} \delta \tag{10}$$

- ***Longitudinal Dynamics***

The longitudinal dynamics describes the motion and behavior of vehicles along their longitudinal axis, which involves acceleration, deceleration, braking, and the associated forces and interactions affecting the vehicle's motion. It directly influences the overall performance and handling characteristics of a vehicle. The ability to accelerate smoothly, maintain stability during braking, and ensure precise control over the vehicle's longitudinal motion are essential for a comfortable and safe driving experience. Consider a vehicle moving on an inclined road, the longitudinal forces acting on the body are shown in Figure 5.

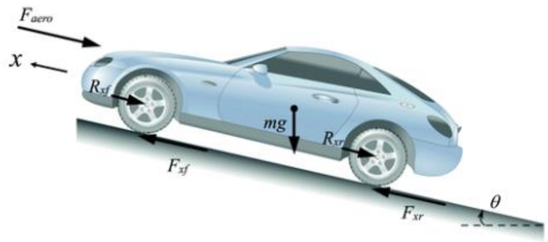

Figure 5. Longitudinal forces acting on the vehicle [15].

While in motion, a vehicle encounters multiple resistive forces due to various factors acting in the opposite direction to the movement. These resistance forces include rolling resistance, aerodynamic resistance, and weight resistance [14] . The force balance along the longitudinal axis leads to the following Eq. (11):

$$m\ddot{x} = F_{xf} + F_{xr} - F_{aero} - R_{xf} - R_{xr} - mg\sin\theta \tag{11}$$

Where Fxf represent the longitudinal tire force at the front tires, Fxr represent is the longitudinal tire force at the rear tires, $Faero$ represent the longitudinal aerodynamic drag force, Rxf represent the the force due to rolling resistance at the front tires, Rxr represent the force due to rolling resistance at the rear tires, m represent the mass of the vehicle, g represent the is the acceleration due to gravity and θ represent the angle of inclination of the road on which the vehicle is traveling.

The equivalent aerodynamic drag force on a vehicle can be represented as [21]:

$$F_{aero} = \frac{1}{2} \rho C_d A_F (V_x + V_{wind})^2 \tag{12}$$

Where, ρ is the mass density of air, C_d is the aerodynamic drag coefficient, A_F is the frontal area of the vehicle, V_x is the longitudinal vehicle velocity and V_{wind} is the wind velocity.

Similarly, the tire force can be expressed as in the following Eq. (13):

$$F_{xf} = C_{\alpha f} \alpha_{xf} \text{ and } F_{xr} = C_{\alpha r} \alpha_{xr} \tag{13}$$

Where $C_{\alpha f}$ and $C_{\alpha r}$ represents the longitudinal tire stiffness parameters of the front

and rear tires respectively, and α_x represents the slip or tire skidding and given as:

$$\alpha_x = \frac{r_{ref} \omega_w - V_x}{V_x} \tag{14}$$

Where R_x is the tire rolling resistance which refers to the force that opposes the motion of the tires as they roll on the road surface. If the road is inclined at an angle α, the rolling resistance R_x can be expressed as:

$$R_x = C_{rr} mgcos(\alpha) \tag{15}$$

Where C_{rr} is the rolling resistance coefficient. It depends on the tire construction, the materials, the air pressure, the vehicle speed, and the road conditions. In addition, m is the vehicle mas and g represent the gravitational acceleration.

- ***Suspension Dynamics***

The suspension system plays an important role in the stability of a vehicle operation [22]. It stands as a pivotal element that profoundly influences the vehicle dynamics and passenger comfort. Suspension systems can be categorized in three main classes: passive, semi-active and active. Passive suspension systems are traditional and common suspension systems that mainly rely on mechanical components like coil spring, shock absorber and connecting elements [16]. On the other hand, active suspension systems use electronic sensors and actuators to actively control vehicles height and damping characteristics. Semi-active suspension systems bridge between passive and active type by using just electronically control dampers.

In this paper, the work is focused on passive suspension systems. Figure 6 shows a schematic of a 2 Degree of Freedom (DOF) quarter car suspension.

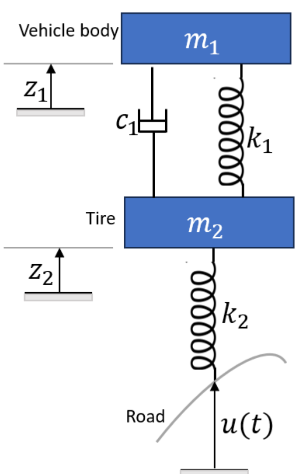

Figure 6. Two-degree of Freedom (DOF) quarter car suspension.

The equations of motion related to mass m_1 and m_2 are given in Eq. (16) and Eq. (17) by:

$$m_1\ddot{z}_1 = -k_1(z_1 - z_2) - c_1(\dot{z}_1 - \dot{z}_2) - F_a \tag{16}$$

$$m_2\ddot{z}_2 = k_1(z_1 - z_2) + c_1(\dot{z}_1 - \dot{z}_2) - k_2\big(z_2 - u(t)\big) - F_a \tag{17}$$

Where m_1 is the body mass, m_2 is the wheel mass, k_1& $k_2$are the stiffness coefficients, $c_1$is the damping coefficient, z_1 is the displacement of the body mass, $z_2$is the displacement of the wheel mass, F_a is the applied external force and $u(t)$ is the road input displacement. The state-space can be obtained from Eq. (16) and Eq. (17) such as:

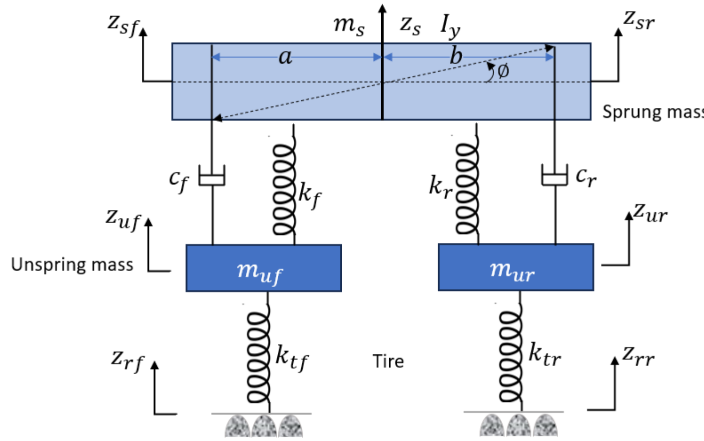

Figure 7. Two DOF half car suspension.

$$\begin{bmatrix} \dot{z}_1 \\ \ddot{z}_1 \\ \dot{z}_2 \\ \ddot{z}_2 \end{bmatrix} = \begin{bmatrix} 0 & 1 & 0 & 0 \\ -\frac{k_1}{m_1} & -\frac{c_1}{m_1} & \frac{k_1}{m_1} & \frac{c_1}{m_1} \\ 0 & 0 & 0 & 0 \\ \frac{k_1}{m_2} & \frac{c_1}{m_2} & -\frac{(k_1+k_2)}{m_2} & -\frac{c_1}{m_2} \end{bmatrix} \times \begin{bmatrix} z_1 \\ \dot{z}_1 \\ z_2 \\ \dot{z}_2 \end{bmatrix} + \tag{18}$$

$$\begin{bmatrix} 0 & 0 \\ \frac{1}{m_1} & 0 \\ 0 & 0 \\ -\frac{1}{m_2} & \frac{k_2}{m_2} \end{bmatrix} \times \begin{bmatrix} F_a \\ u(t) \end{bmatrix} \; and \; \text{y(t)=} \; \begin{bmatrix} 1 & 0 & 1 & 0 \end{bmatrix} \begin{bmatrix} z_1 \\ \dot{z}_1 \\ z_2 \\ \dot{z}_2 \end{bmatrix}$$

A more comprehensive model can be represented through a half car suspension model. It considers a half car, including front and rear body parts. The free body diagram represented in Figure 7 is considered.

With the small angle approximation, the equation of motion related to half body mass m_s is given from Eq. (19) by:

$$\begin{aligned} m_s\ddot{z}_s = &-k_f\big(z_s - z_{uf} - a\emptyset\big) - k_r\big(z_s - z_{ur} + b\emptyset\big) \\ &- c_f\big(\dot{z}_s - \dot{z}_{uf} - a\dot{\emptyset}\big) \\ &- c_r\big(\dot{z}_s - \dot{z}_{ur} + b\dot{\emptyset}\big) \end{aligned} \tag{19}$$

Where: m_s is the body mass, $\emptyset$ represents pitch angle, k_f, k_r, k_{tf}, k_{tr} are the stiffness coefficients, a and b are the distances from the front and rear axle to the center of gravity respectively, z_s is the displacement of the body mass, z_{sf} and z_{sr} are the displacements of the front and rear body masses respectively, z_{uf} and z_{ur} are the displacements of the front and rear wheel masses respectively.

While the equations of motion related to front and rear wheels, $m_{\mu f}$ and $m_{\mu r}$ respectively, are given from Eq. (20) and Eq.(21) as:

$$\begin{aligned} m_{uf}\ddot{z}_{uf} = &\, k_f\big(z_s - z_{uf} - a\emptyset\big) - k_{tf}\big(z_{uf} - z_{rf}\big) \\ &+ c_f\big(\dot{z}_s - \dot{z}_{uf} - a\dot{\emptyset}\big) \end{aligned} \tag{20}$$

$$m_{ur}\ddot{z}_{ur} = k_r(z_s - z_{ur} + b\emptyset) - k_{tr}(z_{ur} - z_{rr}) + c_r(\dot{z}_s - \dot{z}_{ur} + b\dot{\emptyset}) \tag{21}$$

Where m_{uf} and m_{ur} are the front wheel and rear wheel masses while c_f and c_r are the damping coefficients. While z_{rf} and z_{rr} are the road input displacements for the front and the rear wheel respectively.

In the half car model, the moment around the center of gravity must also be considered, such as in (22):

$$I_y\ddot{\emptyset} = ak_f(z_s - z_{uf} - a\emptyset) - bk_r(z_s - z_{ur} + b\emptyset) + ac_f(\dot{z}_s - \dot{z}_{uf} - a\dot{\emptyset}) - bc_r(\dot{z}_s - \dot{z}_{ur} + b\dot{\emptyset}) \tag{22}$$

Where I_y represents the moment of inertia.
The following state matrix is then obtained as in (23):

$$x = [\; z_s \quad \emptyset \quad z_{uf} \quad z_{ur} \quad \dot{z}_s \quad \dot{\emptyset} \quad \dot{z}_{uf} \quad \dot{z}_{ur} \;]^T \tag{23}$$

The state space represented here after is then obtained as in (24) – (28):

$$\dot{x} = \begin{bmatrix} 0 & 0 & 0 & 0 & 1 & 0 & 0 & 0 \\ 0 & 0 & 0 & 0 & 0 & 1 & 0 & 0 \\ 0 & 0 & 0 & 0 & 0 & 0 & 1 & 0 \\ 0 & 0 & 0 & 0 & 0 & 0 & 0 & 1 \\ \multicolumn{4}{c}{-M^{-1}K} & \multicolumn{4}{c}{-M^{-1}C} \end{bmatrix} x + \begin{bmatrix} 0 & 0 \\ 0 & 0 \\ 0 & 0 \\ 0 & 0 \\ \multicolumn{2}{c}{M^{-1}F} \end{bmatrix} u \tag{24}$$

Where:

$$C = \begin{bmatrix} c_f + c_r & bc_r - ac_f & -c_f & -c_r \\ bc_r - ac_f & c_f a^2 + c_r b^2 & ac_f & -bc_r \\ -c_f & ac_f & c_f & 0 \\ -c_r & -bc_r & 0 & c_r \end{bmatrix} \tag{25}$$

$$M = \begin{bmatrix} m_s & 0 & 0 & 0 \\ 0 & I_y & 0 & 0 \\ 0 & 0 & m_{uf} & 0 \\ 0 & 0 & 0 & m_{ur} \end{bmatrix} \tag{26}$$

K=

$$\begin{bmatrix} k_f + k_r & bk_r - ak_f & -k_f & -k_r \\ bk_r - ak_f & k_f a^2 + k_r b^2 & ak_f & -bk_r \\ -k_f & ak_f & k_f + k_{tf} & 0 \\ -k_r & -bk_r & 0 & k_r + k_{tr} \end{bmatrix} \tag{27}$$

$$F = \begin{bmatrix} 0 & 0 \\ 0 & 0 \\ k_{tf} & 0 \\ 0 & k_{tr} \end{bmatrix} \tag{28}$$

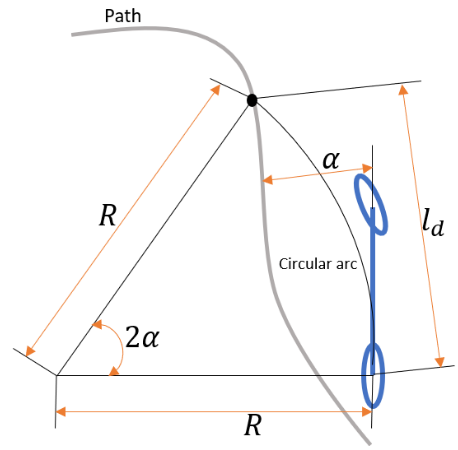

Figure 8. Representation of the principle of the Pure-Pursuit control.

3. Path tracking

A Pure-Pursuit control algorithm for lateral control was implemented with the developed dynamics of the vehicle in order to validate the model. In this section, a brief explanation of this controller is presented.

The pure pursuit technique [23,24] involves a geometric computation of the curvature of a circular arc, linking the position of the rear axle to a target point situated along the path ahead of the vehicle. This objective point is established based on a look-ahead distance l_d extending from the present rear axle position towards the intended path. The target point $(g_x, g_y)$is illustrated in Figure 8.

The steering angle δ of the vehicle can be found using solely the coordinates of the target point and the angle α formed between the vehicle's heading vector and the look-ahead vector, leading to the following equation:

$$\delta = arctan\left(\frac{2L\,sin(\alpha)}{l_d}\right) \tag{29}$$

4. Simulation results and discussion

The vehicle models for both longitudinal and lateral dynamic are implemented in MATLAB/ Simulink as shown in Figure 9. Longitudinal model of the vehicle computed through (11)-(15) is implemented in 'longitudinal vehicle dynamics' block while lateral model represented by (10) is realized in 'lateral vehicle dynamics' block. For the simulation purpose, the parameters of a Tesla Model S were considered. By incorporating these specific parameters, the objective is to conduct comprehensive simulations that closely mimic the real-world scenarios.

A half-car suspension model is also simulated in MATLAB/Simulink. The results are illustrated in Figure 10 (a-b). The suspension system is subjected to two different disturbance signals for the front and rear wheels. These results demonstrate the evolution of body displacement. An examination of the graphs reveals a key principle of this system's operation: the maximum body displacement is half that of the wheel's maximum displacement, highlighting an essential characteristic of the system's behavior.

Vehicle longitudinal and lateral dynamics are tested with various inputs. The initial states of the vehicle are set as $X_0 = 0$, $Y_0 = 0$, $\psi_0 = pi/4$ and $V_{x_0} = 0m/s$. First, the steering angle is fixed as 0 with a lateral speed of $20km/h$. A Proportional-Integral-Derivative (PID) controller is used to achieve desired lateral speed. The tunning proportion, integral and derivative tunning gains are chosen as 20, 4 and 3 respectively. Figure 11 shows the obtained results for this case. Figure 11-a depicts the longitudinal speed while Figure 11-b illustrates the position of the vehicle. Since the steering angle is fixed, the vehicle moved in a straight line. In the second case, the steering angle of the vehicle is kept constant at the value of $\pi/16\ rad$ while keeping the same longitudinal speed profile and initial conditions. The obtained result is shown in Figure 12. As anticipated, the vehicle executed a precise circular motion, showcasing the accuracy of the model.

The path tracking task involved following a predefined path represented by a series of waypoints. The pure-pursuit controller is used to control the lateral motion of the vehicle through appropriate steering commands. The lookahead distance was dynamically adjusted to ensure a smooth tracking. Figure 13 shows the path tracking results along with the trajectory error. One can see that the maximum tracking error is always less than 0.025 meter which indicates that the d esired trajectory is followed quite accurately. Moreover, the simulation results also signify the accuracy of the developed mathematical models and controller.

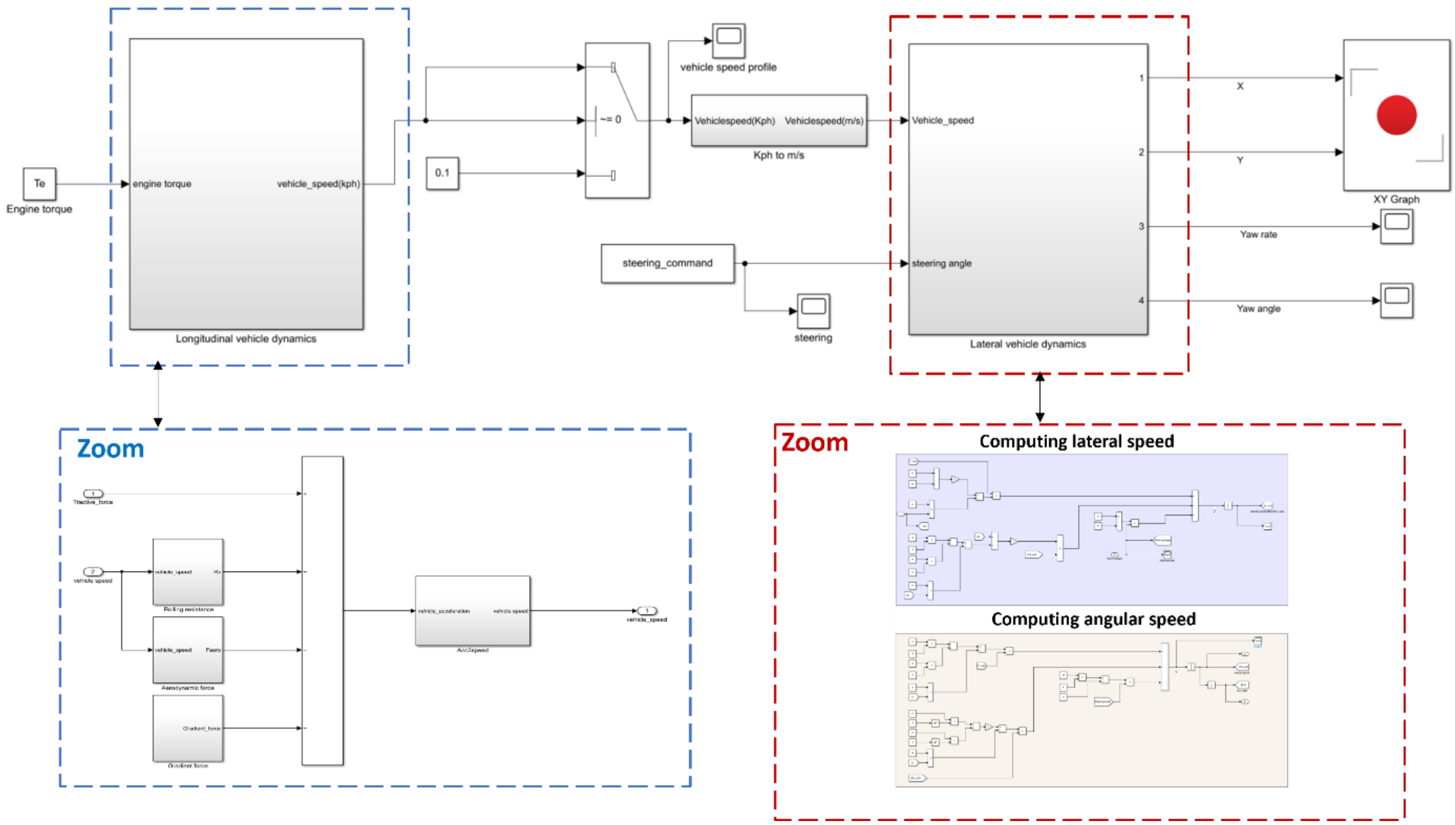

Figure 9. Detailed Simulink model for longitudinal and lateral dynamics.

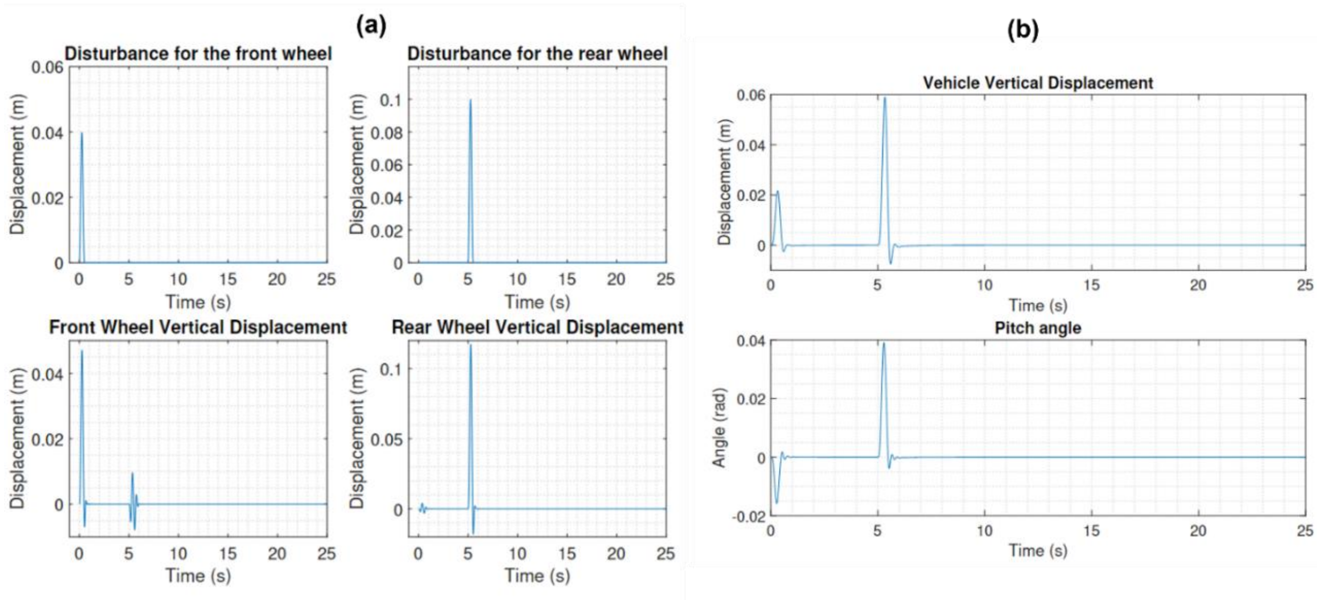

Figure 10. Half-car suspension model results.

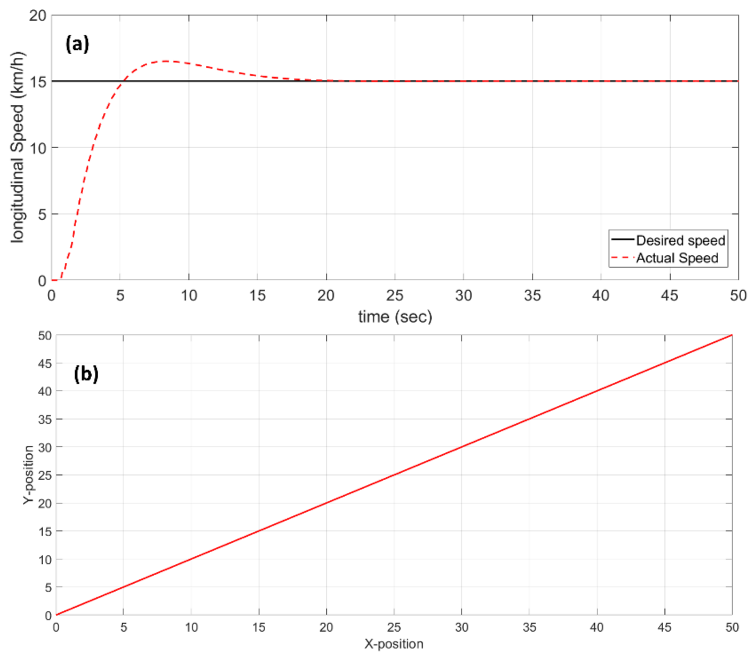

Figure 11. Longitudinal speed (a) and position of the vehicle (b) with a steering angle of zero.

5. Conclusions

In this paper, a mathematical model of vehicle dynamics is developed to describe a vehicle's motion in lateral, longitudinal and vertical directions. These dynamics models are vital for developing and validating algorithms for the vehicles. The models are implemented in MATLAB/Simulink and simulation are carried out with various input signals. The simulation results clearly validate the precision of the developed models, as they consistently mirror the expected vehicle motion. For instance, execution of motion by the vehicle in a straight line or in a circular pattern according to the longitudinal speed and steering angle inputs, the simulation outcomes align seamlessly with the anticipated behaviour. These results underscore the reliability and accuracy of the meticulously developed models, affirming their efficacy in capturing and replicating the dynamic responses of the vehicle in various scenarios. Moreover, a path tracking controller is also integrated to demonstrate the efficiency of the model and verify the accuracy of its derived parameters. Integrating a powertrain model with the vehicle dynamics is anticipated as a future work.

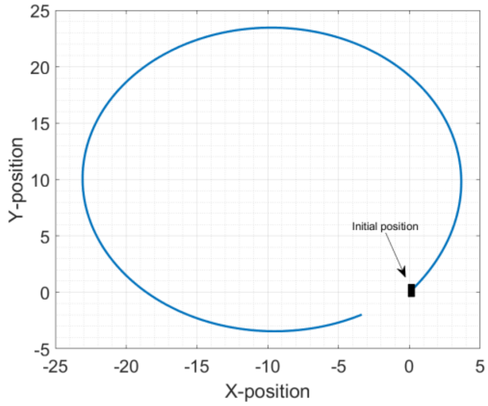

Figure 12. Position of the vehicle with a steering angle of $\boldsymbol{\pi/16}$.

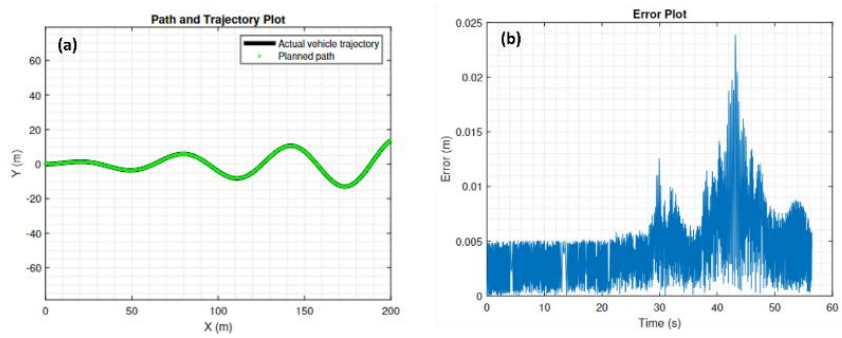

Figure 13. Vehicle motion control (a) path tracking (b) tracking error

Acknowledgment

This work was carried out at Altran Prototypes Automobiles (APA) as a part of the *Intelligence & Innovation Powertrain* project within the Capgemini Engineering Research and Innovation Department.

Conflict of Interest Statement

F.H, A.L and A.S. contributed equally. All authors have given approval to the final version of the manuscript. The authors declare that there is no conflict of interest in the study.

CRediT Author Statement

Fatima Haidar: Writing- review & editing, supervision, project administration & validation. **Abderaouf Laib:** Writing original draft & formal analysis. **Ajwad Syed Ali**: Writing-original draft, methodology, formal analysis, review & validation. **Guillaume Guilbert:** Conceptualization & Validation.

References

1. Hu, C., Wang, Z., Qin, Y., Huang, Y., Wang, J., & Wang, R. (2019). Lane keeping control of autonomous vehicles with prescribed performance considering the rollover prevention and input saturation. IEEE transactions on intelligent transportation systems, 21(7), 3091-3103.
2. Junejo, A. K., Xu, W., Mu, C., Ismail, M. M., & Liu, Y. (2020). Adaptive speed control of PMSM drive system based a new sliding-mode reaching law. IEEE Transactions on Power Electronics, 35(11), 12110-12121.
3. Hasenjäger, M., Heckmann, M., & Wersing, H. (2019). A survey of personalization for advanced driver assistance systems. IEEE Transactions on Intelligent Vehicles, 5(2), 335-344.
4. Zulhilmi, I. M., Peeie, M. H., Eiman, R. I. M., Izhar, I. M., & Asyraf, S. M. (2019). Investigation on vehicle dynamic behaviour during emergency braking at different speed. International Journal of Automotive and Mechanical Engineering, 16(1), 6161-6172.
5. Wada, M., Yoon, K. S., & Hashimoto, H. (2003). Development of advanced parking assistance system. IEEE Transactions on Industrial Electronics, 50(1), 4-17.
6. Liu, L., Lu, S., Zhong, R., Wu, B., Yao, Y., Zhang, Q., & Shi, W. (2020). Computing systems for autonomous driving: State of the art and challenges. IEEE Internet of Things Journal, 8(8), 6469-6486.
7. Yang, S., Lu, Y., & Li, S. (2013). An overview on vehicle dynamics. International Journal of Dynamics and Control, 1, 385-395.
8. Widner, A., Tihanyi, V., & Tettamanti, T. (2022). Framework for vehicle dynamics model validation. IEEE Access, 10, 35422-35436.
9. Farroni, F., Genovese, A., & Sakhnevych, A. (2022). Performance and safety enhancement strategies in vehicle dynamics and ground contact. Applied Sciences, 12(4), 2034.
10. Spiryagin, M., Edelmann, J., Klinger, F., & Cole, C. (2023). Vehicle system dynamics in digital twin studies in rail and road domains. Vehicle System Dynamics, 61(7), 1735-1784.
11. 13. Abe M. (2009) Vehicle Handling Dynamics: theory and application. Vehicle Handling Dynamics: Theory and Application: First Edition. Butterworth-Heinemann.
12. Remirez, C. A. (2015). Active Variable Geometry Suspension for Cars (Doctoral dissertation, Imperial College London).
13. Abe M. (2015) Vehicle Handling Dynamics: theory and application. Vehicle Handling Dynamics: Theory and Application: Second Edition. Butterworth-Heinemann.
14. Karaman, M., & Korucu, S. A. L. İ. H. (2023). Modeling the vehicle movement and braking effect of the hydrostatic regenerative braking system. Engineering Perspective, 3(2), 18-26.
15. Rajamani, R. (2011). Vehicle dynamics and control. Springer Science & Business Media.
16. Alp Arslan T, Aysal FE, Çelik İ, Bayrakçeken H, Öztürk TN. (2022) Quarter Car Active Suspension System Control Using Fuzzy Controller. Engineering Perspective. 4:33–9.
17. Karakaş, O., Şeker, U. B., & Solmaz, H. (2021). Modeling of an electric bus Using MATLAB/Simulink and determining cost saving for a realistic city bus line driving cycle. Engineering Perspective, 1(2), 52-62.
18. Fonseca, L., Olmeda, P., Novella, R., & Valle, R. M. (2020). Internal combustion engine heat transfer and wall temperature modeling: an overview. Archives of Computational Methods in Engineering, 27(5), 1661-1679.
19. Setiawan, Y. D., Roozegar, M., Zou, T., & Angeles, J. (2017). A mathematical model of multispeed transmissions in electric vehicles in the presence of gear shifting. IEEE Transactions on Vehicular Technology, 67(1), 397-408.
20. Min, H., Wu, X., Cheng, C., & Zhao, X. (2019). Kinematic and dynamic vehicle model-assisted global positioning method for autonomous vehicles with low-cost GPS/camera/in-vehicle sensors. Sensors, 19(24), 5430.
21. Da Silva, E. S., Kram, R., & Hoogkamer, W. (2022). The metabolic cost of emulated aerodynamic drag forces in marathon running. Journal of Applied Physiology, 133(3), 766-776.

22. Josee, M., Kazima, S., & Turabimana, P. (2021). Review of semi-active suspension based on Magneto-rheological damper. Engineering Perspective, 2(2), 38-51.
23. Samuel, M., Maziah, M., Hussien, M., & Godi, N. Y. (2018). Control of autonomous vehicle using path tracking: A review. Advanced Science Letters, 24(6), 3877-3879.
24. Samuel, M., Hussein, M., & Mohamad, M. B. (2016). A review of some pure-pursuit based path tracking techniques for control of autonomous vehicle. International Journal of Computer Applications, 135(1), 35-38.